

## Discovery of New Ferroelectrics: $[\text{H}_2\text{dbco}]_2 \cdot [\text{Cl}_3] \cdot [\text{CuCl}_3(\text{H}_2\text{O})_2] \cdot \text{H}_2\text{O}$ (dbco = 1,4-Diaza-bicyclo[2.2.2]octane)

Wen Zhang<sup>†</sup>, Heng-Yun Ye<sup>†</sup>, Hong-Ling Cai<sup>†</sup>, Jia-Zhen Ge<sup>†</sup>, Ren-Gen Xiong<sup>\*†</sup>, and Songping D. Huang<sup>‡</sup>

Ordered Matter Science Research Center, Southeast University, Nanjing 21189, P. R. China and Department of Chemistry, Kent State University, Kent, OH 44242

Received April 7, 2010; E-mail: xiongrg@seu.edu.cn

Ferroelectrics being versatile materials have found many applications in the field of electronics and optics.<sup>1</sup> Reversible electric polarization in response to an external electric field is the essential property for application to nonvolatile memory elements. According to the equation  $D = \epsilon E + P$  ( $D$  = electric displacement,  $\epsilon$  = dielectric constant,  $E$  = electric field, and  $P$  = polarization), if the compound displays ferroelectric properties, the dielectric constant should be nonlinear. In the vicinity of the phase transition point it exhibits an anomaly in response to external stimulus conditions such as temperature, pressure, etc. Also, the structure must fall into 1 of 10 polar point groups ( $C_1$ ,  $C_s$ ,  $C_2$ ,  $C_{2v}$ ,  $C_3$ ,  $C_{3v}$ ,  $C_4$ ,  $C_{4v}$ ,  $C_6$ ,  $C_{6v}$  or 1, 2, 3, 4, 6,  $m$ ,  $mm2$ ,  $3m$ ,  $4mm$ ,  $6mm$ ). Therefore, the distinct Curie temperature ( $T_c$ , ferroelectric phase transition point) in molecular or molecule-based ferroelectrics has been quite an important standard for searching and manifesting new types of ferroelectrics. Generally speaking, the discoveries of most ferroelectrics can be first manifested through a dielectric anomaly near the  $T_c$ . Furthermore, the ordered and disordered structural states can exist in low and high temperature environmental conditions, which stand for low and high symmetry. During the change process from a disordered one (high symmetry) to the ordered state (low symmetry) the symmetry breaking phenomenon usually occurs. This turning point from the ordered state to a disordered one may be the phase transition point, and near the point most physical properties such as dielectric constant will sharply change. Consequently, the first task is to search and discover the dielectric constant anomaly in response to temperature stimulus.

In the course of investigations of molecule-based ferroelectrics,<sup>2–5</sup> we have successfully found that, in the replacement of  $\text{NH}_4^+$  or  $\text{MeNH}_3^+$  and  $\text{SO}_4^{2-}$  by  $\text{H}_2\text{dbco}$  ( $\text{H}_2\text{dbco}$  = 1,4-diaza-bicyclo[2.2.2]-octane) and  $\text{SeO}_4^{2-}$ , a new ferroelectrics  $[(\text{H}_2\text{dbco})\text{Cu}(\text{H}_2\text{O})_6(\text{SeO}_4)_2]$  has been formed.<sup>5</sup> It undergoes a phase transition ( $T_c = -140^\circ\text{C}$ ) from a high temperature paraelectric phase with a space group of  $P2_1/m$  to a low temperature ferroelectric one with a space group of  $P2_1$ . During the change process from the high temperature phase to the low one, the symmetry breaking occurs; i.e. four symmetry elements decrease into two symmetry elements. This is a successful combination of a variation-temperature-crystal engineering strategy and Landau phase transition theory in the application of ferroelectrics design.

Following this idea, during the investigation of temperature-dependent dielectric constant measurements on the powdered  $[\text{H}_2\text{dbco}]_2 \cdot [\text{Cl}_3] \cdot [\text{CuCl}_3(\text{H}_2\text{O})_2] \cdot \text{H}_2\text{O}$  (**1**), it is surprisingly found that at approximately  $-23^\circ\text{C}$  the dielectric constant displays an anomaly and sharply increases from *ca.* 9 to 20, approximately a double increase, indicating that the phase transition may be a ferroelectric phase transformation. Herein we report the different temperature crystal structures, differential scanning calorimetry

(DSC), specific heat ( $C_p$ ), single crystal temperature-dependent dielectric constant, and ferroelectric property of **1**. As we are aware, it is the first molecular metal coordination compound ferroelectrics with a large dielectric response involving a 2 orders of magnitude enhancement and distinct Curie phase transition point.

DSC measurement is a common method for detecting whether there is a phase transition occurring in response to the temperature. For **1**, there is a heat anomaly observed at *ca.* 230 K upon cooling or *ca.* 235 K upon warming. The small heat hysteresis of 5 K and a round-like peak indicates a reversible phase transition occurrence with a second-ordered feature, as shown in Figure 1.

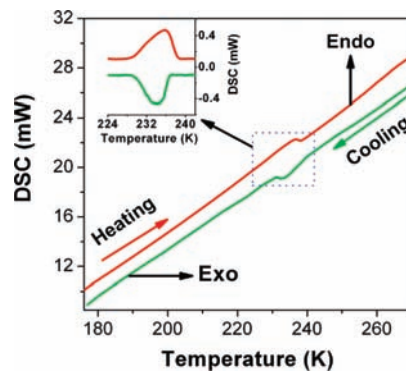


Figure 1. DSC curve of **1**.

It is well-known that the shape of the specific heat plot will further confirm whether there is a phase transition occurring and the phase transition character. Figure 2 shows that a round-like peak appears at *ca.* 234 K, definitely manifesting the presence of a phase transition as a typical second-order one, like that of triglycine sulfate (TGS). The  $\Delta S$  value equals  $1.8366 \times 10^{-3} \text{ J/(g K)}$ . According to  $\Delta S = R \ln N$ , the  $N$  value is estimated to be *ca.* 1.2, showing an ordered–disordered feature.<sup>6</sup>

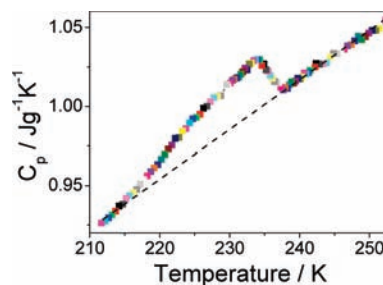
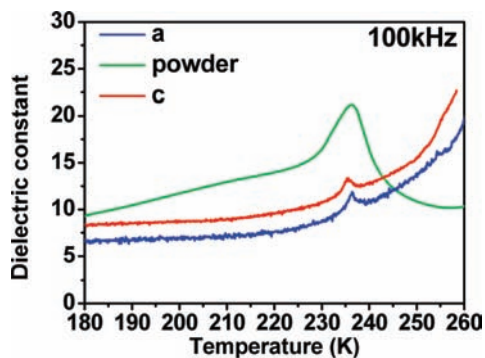


Figure 2. Temperature dependence of specific heat of **1**.

As mentioned above, the physical property will sharply change near the phase transition point and the changing magnitude will be relative to the character of the phase transitions, i.e. common phase transition,

<sup>†</sup> Southeast University.

<sup>‡</sup> Kent State University.



**Figure 3.** Temperature-dependence of dielectric constant of **1** in which a (blue line), powdered (green line), and c (red line) stand for approximately along the *a*-axis, powdered samples, and approximately along the *c*-axis, respectively. The measured frequency is fixed at 100 kHz. The electrode preparations used graphite-conducting glue and copper wires.

ferroelastic, or ferroelectric. Figure 3 preliminarily shows that the phase transition of **1** belongs to a ferroelectric one because, usually, the dielectric constant changes with an approximately double increase from a low to high temperature process for a powdered sample.

The temperature-dependent dielectric constant measurement along the polar axis further confirms that the permittivity change reaches a large value (over 2000 at 1 kHz) with a 2 orders of magnitude enhancement, suggesting that the phase transition should be a ferroelectric one. The dielectric constant should obey the Curie–Weiss law ( $\epsilon = \epsilon_0 + C/(T - T_0)$ ) above the transition point. The inserted plot, fitted by the reciprocal dielectric susceptibility ( $\epsilon^{-1}$ ) vs temperature, shows that near the phase transition point the curve is almost linear and the Curie–Weiss constant ( $C_{\text{para}}$ ) is estimated to be  $1.7 \times 10^3$  K falling into the magnitude range of typical molecular ferroelectrics such as TGS ( $3.2 \times 10^3$ ),  $\text{NaNNO}_2$  ( $5.0 \times 10^3$ ),  $\text{KH}_2\text{PO}_4$  ( $3.3 \times 10^3$ ), and Rochelle salt ( $2.2 \times 10^3$ ). To the best of our knowledge, this is the first example of metal complex type ferroelectrics with such a high dielectric constant over the  $1 \times 10^3$  range in known complex ferroelectrics such as  $\text{NH}_4\text{M}(\text{SO}_4)_2 \cdot 12\text{H}_2\text{O}$ ,  $\text{MeNH}_3\text{M}(\text{SO}_4)_2 \cdot 12\text{H}_2\text{O}$  ( $\text{M} = \text{Fe}^{3+}$ ,  $\text{Al}^{3+}$ ,  $\text{V}^{3+}$ ,  $\text{Cr}^{3+}$ ,  $\text{In}^{3+}$ , and  $\text{Ga}^{3+}$ ), and  $\text{K}_4\text{M}(\text{CN})_6 \cdot 3\text{H}_2\text{O}$  ( $\text{M} = \text{Fe}^{2+}$ ,  $\text{Mn}^{2+}$ ,  $\text{Ru}^{2+}$ , and  $\text{Os}^{2+}$ ).<sup>7</sup> On the other hand, below  $T_c$ , the Curie–Weiss constant  $C_{\text{ferro}}$  is also estimated to be  $2.14 \times 10^3$  K. Thus the ratio of  $C_{\text{para}}$  to  $C_{\text{ferro}}$  is estimated to be 0.81, a typical feature of a second-order phase transition. Finally we can obtain  $T_0 = 234$  K, being consistent with that of  $T_c$ , suggesting this phase transition is a

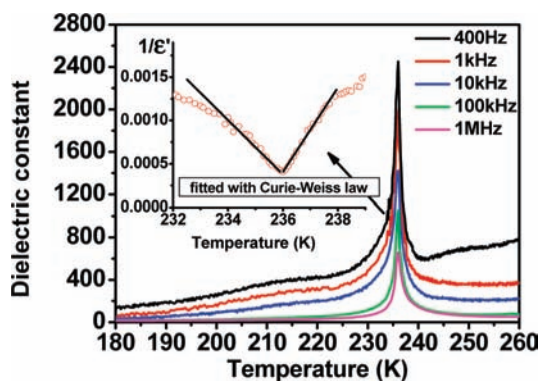


**Figure 4.** Dielectric constant ( $\epsilon_b$ ) of **1** along the *b*-axis, as a function of temperature, measured at different frequencies. Inset figure is the reciprocal dielectric susceptibility ( $1/\epsilon$ ) vs temperature curve, where  $1/\epsilon$  follows the Curie–Weiss law:  $1/\epsilon = C/(T - T_0)$  within a narrow temperature range above the Curie point ( $T_0 \approx 234$  K), indicating the phase transition feature should be second-order because there no latent heat occurred in a typical second-order phase transition.

second-order one as shown in Figure 4. Apparently, the dielectric constant as a function of temperature approximately along two other nonpolar axes shows a very small anomaly (Figure 3), consistent with that found in  $(\text{NH}_4)_2\text{SO}_4$  and  $(\text{NH}_4)_4\text{BeF}_4$  in which their dielectric constants are also temperature dependent.<sup>7</sup>

The crystal structure of **1** at room temperature reveals that it belongs to an orthorhombic crystal system with a centrosymmetric space group of  $Pnma$  and nonpolar point group  $D_{2h}$ , which belongs to a paraelectric state and consistent with that reported by Willett et al.<sup>8,9</sup> The asymmetric unit of the solid state structure of **1** at room temperature is composed of two  $[\text{H}_2\text{dbco}]^{2+}$  cations, three  $\text{Cl}^-$  anions that are hydrogen-bonded to the  $[\text{H}_2\text{dbco}]^{2+}$  cations, a discrete  $[\text{CuCl}_3(\text{H}_2\text{O})_2]^-$  anion in which the central copper(II) ion lies on a mirror plane in the crystal and is coordinated by three  $\text{Cl}^-$  anions and two  $\text{H}_2\text{O}$  molecules, and one lattice  $\text{H}_2\text{O}$  molecule. Furthermore, the coordination geometry around the Cu(II) is best described as distorted trigonal bipyramidal with two oxygen atoms occupying the axial positions. More interestingly, the disordered feature of one of the two  $[\text{H}_2\text{dbco}]^{2+}$  cations shown in Figure 5 indicates that, at room temperature, **1** belongs to a high symmetric and more disordered status, which will change to a low symmetric and more ordered status upon decreasing the temperature below the phase transition point as confirmed by low temperature structure determination.

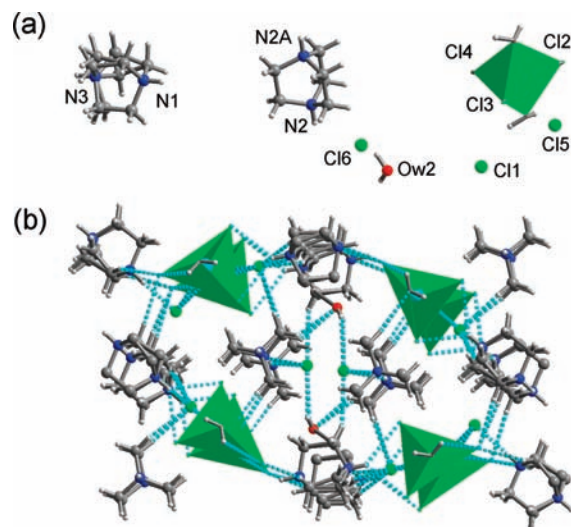


**Figure 5.** (a) Asymmetric unit of **1** at room temperature showing that one of the two  $[\text{H}_2\text{dbco}]^{2+}$  cations displays a disordered feature. (b) Packing view along the *b*-axis.

After the temperature decreases down to  $-80$  °C, the crystal structure determination of **1** reveals that it still belongs to an orthorhombic crystal system but with a noncentrosymmetric space group of  $Pna2_1$  and a polar point group of  $C_{2v}$ , which belongs to a ferroelectric phase. In the solid state structure of **1** under the  $-80$  °C temperature the disordered  $[\text{H}_2\text{dbco}]^{2+}$  cation clearly becomes more ordered as shown in Figure 6 and the central Cu atom in the

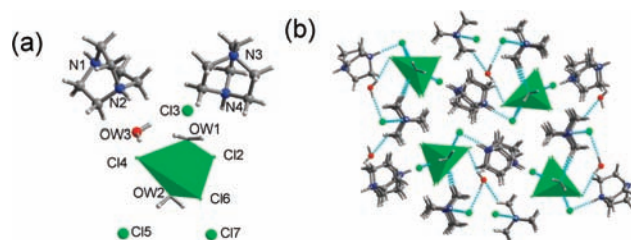


**Figure 6.** (a) Asymmetric unit of **1** at  $-80$  °C where the disordered  $[\text{H}_2\text{dbco}]^{2+}$  cation becomes more ordered. (b) Packing view along the *b*-axis.

big anion  $[\text{Cu}(\text{Cl}_3)(\text{H}_2\text{O})_2]^-$  still adopts a slightly distorted trigonal bipyramidal coordinated environment.

After the temperature continuously decreases down to  $-180^\circ\text{C}$ , the crystal structure (see Supporting Information) still remains the same crystal system (orthorhombic) as that found in  $-80^\circ\text{C}$ . Thus, in the cooling process from high temperature to low temperature, symmetry breaking takes place with an Aizu notation of  $mmmFmm2$ ; that is, the eight symmetric elements ( $e$ ,  $C_2$ ,  $C_2'$ ,  $C_2''$ ,  $i$ ,  $\sigma_h$ ,  $\sigma_v$ ,  $\sigma_v'$ ) at the paraelectric phase (above 236 K) are halved into four ( $e$ ,  $C_2$ ,  $\sigma_v$ ,  $\sigma_v'$ ) owing to the loss of the symmetric elements  $C_2'$ ,  $C_2''$ ,  $i$ , and  $\sigma_h$ , which is attributed to a typical second-order feature according to Landau phase transition theory. This kind of ferroelectric phase transition is reminiscent of  $(\text{NH}_4)_2\text{SO}_4$  and  $(\text{NH}_4)_4\text{BeF}_4$  undergoing a ferroelectric phase transition from  $Pnma$  to  $Pna2_1$ . For a stress-free crystal, an expansion of the Gibbs free energy ( $G$ ) can be written as follows:  $G(\eta) = G_0 + (1/2)A\eta^2 + (1/4)B\eta^4 + (1/6)C\eta^6 + \dots$ . Near the phase transition temperature ( $T_c$ ), the  $\eta$  can be determined by minimizing the truncated Gibbs potential,  $\partial G/\partial\eta = A\eta + B\eta^3$ . Under the limited conditions, we can obtain  $P_s = (2\varepsilon_0\Delta SC)^{1/2}$ , where  $P_s$ ,  $\varepsilon_0$ ,  $\Delta S$ , and  $C$  stand for spontaneous polarization, vacuum permittivity, entropy change, and Curie–Weiss constant, respectively. For **1**, at 400 Hz,  $C$  equals  $2.023 \times 10^3 \text{ K}$  and  $P_s$  is estimated to be  $1.04 \mu\text{C cm}^{-2}$  which is basically comparable to the experimental value.<sup>10</sup>

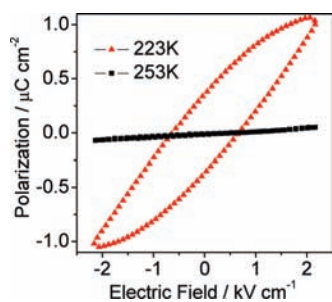


**Figure 7.** Dielectric hysteresis loop of **1** measured at the frequency of 400 Hz in which we used the self-designed ferroelectric tester using a Sawyer–Tower circuit (see Supporting Information).

The hysteresis loop can be recorded with a simple Sawyer–Tower circuit at 400 Hz. On cooling from  $25^\circ\text{C}$  (room temperature), the loop looks like a line which may only contain two components consisting of dielectric and conducting contributions, but no ferroelectric part, indicating a typical paraelectric phase (Figure 7). In this state, according to the above-mentioned equation ( $D = \varepsilon E + P$ ), the polarization  $P$  should be linear to the electric field. With the temperature decreasing, just below the  $T_c$ , the line suddenly opens and becomes a typical ferroelectric loop. Such a ferroelectric loop can be seen only in a very limited temperature range of a few degrees just below the  $T_c$ . The spontaneous polarization is estimated to be *ca.*  $1.1 \mu\text{C cm}^{-2}$  at approximately  $-24^\circ\text{C}$ , which is in good agreement with the calculated value. Below  $T_c$ , the coercive field  $E$  also increases steeply with the temperature decrease, which makes it impossible for one to observe a good ferroelectric loop. In this case,  $E_c$  is approximately  $1.0 \text{ kV cm}^{-1}$ . Moreover, the  $P_s$  is transformed to the dipole moment ( $\mu_s$ ) per formula unit, i.e.

$$\mu_s = P_s/N = 1.0438 \mu\text{C cm}^2/1.7852 \times 10^{27} \text{ m}^{-3} = 5.847 \times 10^{-30} \text{ C m}$$

Using the density of dipoles ( $Z = 4$ ,  $V = 2240.6 \text{ \AA}^3$ ,  $N = Z/V =$

$1.7852 \times 10^{27} \text{ m}^{-3}$ ) and in relation to the observed large Curie constant ( $C$ ), it is found that the effective paraelectric moment ( $\mu_c$ ) can be estimated from the following equation:

$$\begin{aligned} \mu_c^2 &= Ck_B\varepsilon_0/N = 2023 \text{ K} \times 1.38065 \times 10^{-23} \text{ m}^2 \cdot \text{kg} \cdot \text{s}^{-2} \text{ K}^{-1} \times \\ &8.854 \times 10^{-12} \text{ F m}^{-1}/1.7852 \times 10^{27} \text{ m}^{-3} = \\ &138.526 \times 10^{-60} \text{ m}^4 \cdot \text{kg} \cdot \text{s}^{-2} \text{ F} \end{aligned}$$

where  $k_B$  and  $\varepsilon_0$  are the Boltzmann constant and permittivity of vacuum, respectively. Furthermore,  $\mu_c^2 = 138.526 \times 10^{-60} \text{ m}^4 \cdot \text{kg} \cdot \text{s}^{-2} \text{ F} = 138.526 \times 10^{-60} \text{ m}^2 \text{ J F} = 138.526 \times 10^{-60} \text{ m}^2 \text{ C}^2$  where the physical unit transformation can be done according to  $1 \text{ J} = 1 \text{ N m} = \text{kg ms}^{-2} \text{ m} = 1 \text{ C V} = \text{C(C/F)}$ . Thus,  $\mu_c$  is equal to  $11.77 \times 10^{-30} \text{ C m}$ , while the ratio  $\mu_c/\mu_s$  is equal to 2 which is a typical value for ferroelectrics with the proper ferroelectric transition in which the spontaneous polarization stands for the order parameter in Landau theory.<sup>11</sup>

In conclusion, the present work has proved an effective way for exploration of new ferroelectrics based on a five-coordinated divalent metal through the combination of crystal engineering and Landau phase transition theory.

**Acknowledgment.** This work was supported by the National Natural Science Foundations of China (20973037, 90922005, and 20931002) and Jiangsu Province NSF (BK2008029). X.R.G. thanks Chen Fan, Fu Da-Wei, Hang Tian, and Dr. Zhang Yi for their synthetic work, DSC and  $C_p$  measurement, and illustration.

**Supporting Information Available:** The powdered XRD patterns, IR and crystal structure at  $-180^\circ\text{C}$ , dielectric constants in powdered state, other two nonpolar axes as a function of temperature, X-ray crystallographic cif file. This material is available free of charge via the Internet at <http://pubs.acs.org>.

## References

- (1) (a) Scott, J. F.; Araujo, C. A. *Science* **1989**, *246*, 1400. (b) Lee, H. N. H.; Christen, M.; Chirsholm, M. F.; Rouleau, C. M.; Lowndes, D. H. *Nature* **2005**, *433*, 395.
- (2) Zhang, W.; Ye, H.-Y.; Xiong, R.-G. *Coord. Chem. Rev.* **2009**, *253*, 2980.
- (3) Zhang, W.; Xiong, R.-G.; Huang, S.-P. D. *J. Am. Chem. Soc.* **2008**, *130*, 10468.
- (4) Ye, H.-Y.; Fu, D.-W.; Zhang, Y.; Zhang, W.; Xiong, R.-G.; Huang, S. D. *J. Am. Chem. Soc.* **2009**, *131*, 42.
- (5) Zhang, W.; Chen, L.-Z.; Xiong, R.-G.; Nakamura, T.; Huang, S.-P. D. *J. Am. Chem. Soc.* **2009**, *131*, 12544.
- (6) Jain, P.; Ramachan, V.; Clark, R. J.; Zhou, H. D.; Toby, R. H.; Dalal, N. S.; Kroto, H.; Cheetham, A. K. *J. Am. Chem. Soc.* **2009**, *131*, 13625.
- (7) Jona, F.; Shirane, G. *Ferroelectric Crystals*; Pergamon Press: New York, 1962.
- (8) Crystal data for **1** at 293 K:  $\text{C}_{12}\text{H}_{34}\text{CuN}_4\text{O}_3\text{Cl}_6$ ,  $M_r = 558.67$ , orthorhombic,  $Pnma$ ,  $a = 15.209(6) \text{ \AA}$ ,  $b = 7.457(3) \text{ \AA}$ ,  $c = 20.158(8) \text{ \AA}$ ,  $V = 2286.1(15) \text{ \AA}^3$ ,  $Z = 4$ ,  $D_c = 1.623 \text{ Mg m}^{-3}$ ,  $R_1 (I > 2\sigma) = 0.0554$ ,  $wR_2 = 0.1729$ ,  $\mu = 1.623 \text{ mm}^{-1}$ ,  $S = 1.332$ . **1** at 193 K:  $\text{C}_{12}\text{H}_{34}\text{CuN}_4\text{O}_3\text{Cl}_6$ ,  $M_r = 558.67$ , orthorhombic,  $Pna2_1$ ,  $a = 15.1267(9) \text{ \AA}$ ,  $b = 20.0939(13) \text{ \AA}$ ,  $c = 7.4239(5) \text{ \AA}$ ,  $V = 2256.5(2) \text{ \AA}^3$ ,  $Z = 4$ ,  $D_c = 1.644 \text{ Mg m}^{-3}$ ,  $R_1 (I > 2\sigma) = 0.0363$ ,  $wR_2 = 0.0821$ ,  $\mu = 1.699 \text{ mm}^{-1}$ ,  $S = 1.103$ , Flack value = 0.509(17). **1** at 93 K:  $\text{C}_{12}\text{H}_{34}\text{CuN}_4\text{O}_3\text{Cl}_6$ ,  $M_r = 558.67$ , orthorhombic,  $Pna2_1$ ,  $a = 15.0638(8) \text{ \AA}$ ,  $b = 20.0568(15) \text{ \AA}$ ,  $c = 7.4158(5) \text{ \AA}$ ,  $V = 2240.5(3) \text{ \AA}^3$ ,  $Z = 4$ ,  $D_c = 1.656 \text{ Mg m}^{-3}$ ,  $R_1 (I > 2\sigma) = 0.0306$ ,  $wR_2 = 0.0836$ ,  $\mu = 1.711 \text{ mm}^{-1}$ ,  $S = 1.144$ , Flack value = 0.510(13). Normally, the Flack value is larger than or approximately equal to 0.5, probably suggesting that the value of the Flack parameter is based on how many Friedel's pairs you used in your refinement. So, the particular crystal is twinned by inversion. For  $-80^\circ\text{C}$ ,  $\sim 2279$  Friedel's pairs were used while, for  $-180^\circ\text{C}$ , 2356 Friedel's pairs were approximately used.<sup>5</sup>
- (9) Wei, M.; Willett, R. D. *Inorg. Chem.* **1996**, *35*, 6381.
- (10) Mitsuhi, T.; Tatsuzaki, I.; Nakamura, E. *An Introduction to the Physics of Ferroelectrics*; Grodon and Breach Science Publishers Inc.: New York, 1976; p 10016.
- (11) (a) Horiuchi, S.; Kumai, R.; Tokunaga, Y.; Tokura, Y. *J. Am. Chem. Soc.* **2008**, *130*, 13382. (b) Ye, H.-Y.; Chen, F.; Xiong, R.-G. *Acta Crystallogr.* **2010**, B66 (in press, HW5007).

JA102573H